Near-Threshold Fatigue Crack Growth Behavior in Copper

PETER K. LIAW, T. R. LEAX, R. S. WILLIAMS, and M. G. PECK

Near-threshold fatigue crack growth rate data were developed in annealed, quarter-hard, and full-hard copper at various load ratios, ($R = \sigma_{min}/\sigma_{max}$). Increasing the R value decreases the resistance to threshold crack growth. At a fixed value of R, annealed copper has the slowest near-threshold crack propagation rate while full-hard copper has the fastest crack growth rate. Waveform (sine and triangle) and specimen geometry (WOL, CT, and CCT) do not appear to affect the rates of near-threshold crack propagation. The influences of load ratio and material strength on threshold crack growth behavior can be rationalized by crack closure.

I. INTRODUCTION

THE fracture mechanics approach to the evaluation of fatigue crack growth behavior provides an extremely valuable tool for the development of rational design criteria useful in assessing structural integrity and preventing failure. The use of the preexisting defect tolerant approach in fatigue life prediction can reduce or eliminate the crack initiation phase of a fatigue crack which may account for a very large percentage of the cyclic life. However, at very low stress intensity ranges, preexisting cracks either grow at very low rates or do not grow at all under cyclic loading. Since fatigue crack growth behavior near the threshold is extremely important in applications involving very long life considerations, it is necessary to develop these data in structural materials.

This paper presents the results of an evaluation of the near-threshold fatigue crack growth rate behavior in commercially pure copper. The effects of material condition (annealed, quarter-hard, and full-hard) and load ratio were investigated in detail. The influences of waveform and specimen geometry on slow crack propagation rates were also considered. Auger analysis was used to examine the effects of oxide deposits on threshold crack growth behavior. In particular, the role of crack closure during near-threshold fatigue crack propagation was emphasized.

II. MATERIAL

Near-threshold fatigue crack growth tests in air were performed in ETP (Electrolytic Tough Pitch) copper with 99.95 pct purity. Three material conditions were characterized: annealed, quarter-hard, and full-hard. Quarter-hard and full-hard specimens were cold-rolled to 11 pct and 31 pct reduction in thickness, respectively. To produce annealed specimens, quarter-hard materials were heat-treated at 550 °C for one hour. The mechanical properties are shown in Table I.

While annealed copper shows a considerable amount of cyclic hardening, quarter-hard and full-hard copper show cyclic softening. Even though the annealed and quarter-hard (full-hard) materials have significantly different monotonic yield strengths, both have approximately the same order of cyclic yield strength. This appears to be consistent with Laird and Feltner's[1] finding that a material of high stacking fault energy possesses a unique cyclic stress and strain curve regardless of the previous deformation history. Interestingly, the three materials have nearly the same ultimate tensile strength; see Table I.

III. EXPERIMENTAL TECHNIQUE

Near-threshold fatigue crack growth tests in annealed and full-hard copper were performed using WOL (wedge-open-loading) compact toughness specimens. The experiments in the quarter-hard material were conducted with WOL, CT (compact tension), and CCT (center-cracked) specimens to investigate the effect of specimen geometry on slow crack propagation behavior. The dimensions of the specimens are listed in Table II which shows a large difference in specimen size for the three geometries. The notch in each specimen was oriented along the rolling direction in quarter-hard and full-hard specimens. The tests were conducted in air at load ratios (R) of 0.1, 0.3, 0.5, and 0.7. Sinusoidal and triangular waveforms were used at a frequency of 100 Hz. All of the specimens were precracked in accordance with ASTM Standard E647.

The testing system is a closed-loop, electrohydraulic MTS machine interfaced with a PDP 11/34A computer. The details of the computerized threshold fatigue crack propagation test have been reported elsewhere.[2] Briefly, the near-threshold fatigue crack growth rates were developed by automatically reducing the stress intensity range, ΔK, according to Eq. [1], as suggested by Saxena *et al*,[3]

$$\Delta K = \Delta K_0 e^{c(a-a_0)} \qquad [1]$$

where ΔK_0 is the initial stress intensity range, a is the crack length, a_0 is the initial crack length, and c is a constant with a unit of reciprocal length. In this study, the value of c is equal to -0.098 mm^{-1} which is suitable for copper.[2]

Crack length was determined using the elastic compliance method.[4] Visual measurements of crack lengths were in good agreement with those determined by the compliance technique.[2] The ΔK expression for each specimen geometry can be found in Reference 4.

Briefly, the logic used by the automated system can be divided into three steps. First, the fatigue crack length was

PETER K. LIAW, Senior Engineer, and M. G. PECK, Research Technician, are both with Westinghouse Research and Development Center, Materials Engineering Department. T. R. LEAX is Advanced Engineer, Westinghouse Steam Turbine Generator Division, and R. S. WILLIAMS is Senior Engineer, Westinghouse Research and Development Center, Physical Metallurgical Department, Pittsburgh, PA 15235.

Manuscript submitted October 13, 1981.

ISSN 0360-2133/82/0911-1607$00.75/0
© 1982 AMERICAN SOCIETY FOR METALS AND THE METALLURGICAL SOCIETY OF AIME

Table I. Mechanical Properties of ETP Copper

Material	0.2 Pct Offset Monotonic Yield Strength (MPa)	Ultimate Tensile Strength (MPa)	0.2 Pct Offset Cyclic Yield Strength* (MPa)	Elongation (Pct)	Grain Size** (μm)
Annealed	67	263	134	48	65
Quarter-hard	188	246	162	27	45
Full-hard	194	249	177	26	25

*The cyclic yield strength was determined by the incremental step test.
**Grain size perpendicular to the rolling direction.

determined by the compliance. Second, the value of decreased ΔK was then calculated by Eq. [1]. Third, the applied load was determined by using the ΔK expression depending on the specimen geometry.[4] The above three steps were repeated until the fatigue crack propagation rate reached the threshold. This computerized test can be performed completely unattended after the operator sets up the test. As compared to the manual load-shedding method which is often used in near-threshold crack growth tests, the present system reduces costly labor and testing time considerably. Furthermore, data acquisition and analysis were automated to give instantaneous information on crack growth rates during the test. The rate of crack propagation, da/dN, was determined by fitting a polynomial through seven consecutive a *vs* N (cycle) data points, and was defined as the derivative of the polynomial at the middle point.

IV. RESULTS

A. *Effect of Load Ratio*

The influence of R values on near-threshold crack growth rates in annealed, quarter-hard, and full-hard ETP copper is shown in Figures 1(a) to (c). For these materials, increasing the R ratio increases the rate of slow crack growth. Similar behavior has been noted in other alloying systems.[5-10] As the crack propagation rate decreases, the difference in growth rates associated with R values becomes larger. Again, this behavior is characteristic of near-threshold crack growth rate performance. Note that in Figures 1(a) to (c) the annealed specimen with the lowest monotonic yield strength exhibits the greatest sensitivity to the R ratio effect on the rate of near-threshold crack propagation. Quarter-hard copper seems to be more sensitive to the influence of R on threshold behavior than full-hard copper. Thus, it appears that as the strength increases in copper, the effect of load ratio on near-threshold crack propagation rates decreases. Ritchie[7] also reported that increasing the strength in tempered martensitic steels decreased the threshold growth rate dependence on the R ratio.

Table II. Specimen Geometry

Specimen	Width (mm)	Height (mm)	Thickness (mm)	Notch Length (mm)
WOL	81.3	63.0	6.35	32.4
CT	32.2	31.0	9.00	15.0
CCT	75.5	228.3	6.35	27.0

B. *Effects of Waveform and Specimen Geometry*

Waveform (sinusoidal or triangular) does not affect crack growth rates in annealed, quarter-hard, and full-hard copper as shown in Figure 2. Similar results were noted in an RR 58 T651 aluminum alloy.[11] For the three specimen geometries studied, WOL, CT, and CCT, there is no significant difference in the rates of near-threshold crack propagation for quarter-hard copper at $R = 0.1$ (Figure 3). Similar behavior was also found in aluminum alloys.[11,12] Thus, based on linear-elastic fracture mechanics, the threshold fatigue crack growth rate data developed with various specimen geometries can be interchanged and utilized in engineering design.

C. *Comparison of Near-Threshold Crack Propagation Behavior*

The rates of slow crack growth in annealed, quarter-hard, and full-hard copper are compared in Figures 4(a) to (c). It appears that as the near-threshold crack propagation rates decrease, the difference in growth rates among the three materials increases. At threshold levels and for a given value of crack growth rate, the corresponding ΔK in full-hard copper is much smaller than that in annealed or quarter-hard copper (Figures 4(a) to (b)). For a fixed value of ΔK, quarter-hard copper has a faster threshold crack propagation rate than annealed copper at $R = 0.1$ and 0.3. This suggests that increasing the copper's strength by cold working decreases the resistance to slow fatigue crack growth. Similar results were also reported in steels.[13] Figures 4(a) to (c) showed that increasing R values seemed to reduce the difference in crack propagation rates among annealed, quarter-hard, and full-hard copper. Interestingly, at $R = 0.5$, the near-threshold crack growth rates in annealed and quarter-hard specimens are essentially identical.

To define operationally the value of the threshold stress intensity range, ΔK_{th}, low rates of crack propagation ranging from approximately 3.5×10^{-10} to 6×10^{-11} m per cycle were fitted by a least-squares regression and the value of ΔK corresponding to a crack growth rate of 10^{-10} m per cycle was taken to be ΔK_{th}. Table III lists ΔK_{th} for the three materials. The value of ΔK_{th} in full-hard copper at $R = 0.1$ is close to the literature value[10] of 2.5 MPa $\sqrt{m}$ at $R = 0$.

D. *Fractography*

The fracture surfaces were carefully examined and the pertinent results are summarized as follows:

(a) For each material investigated, it was noted that as the fatigue crack growth rate approached the threshold, the

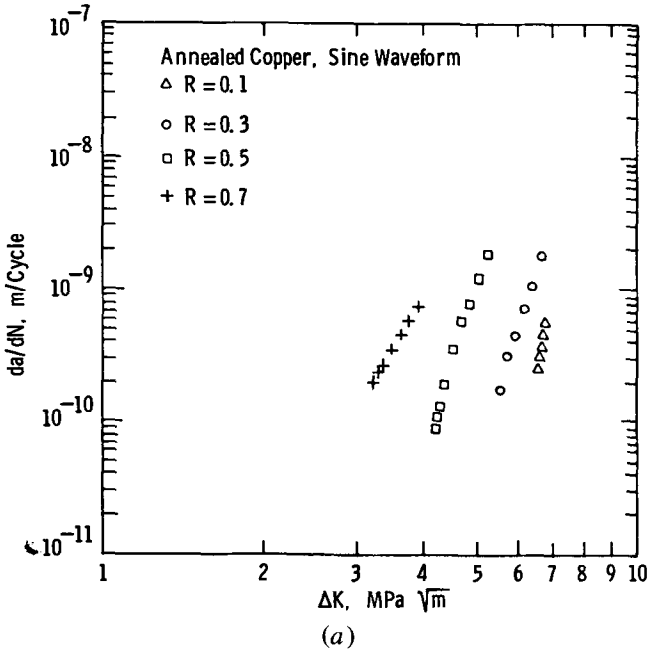

(a)

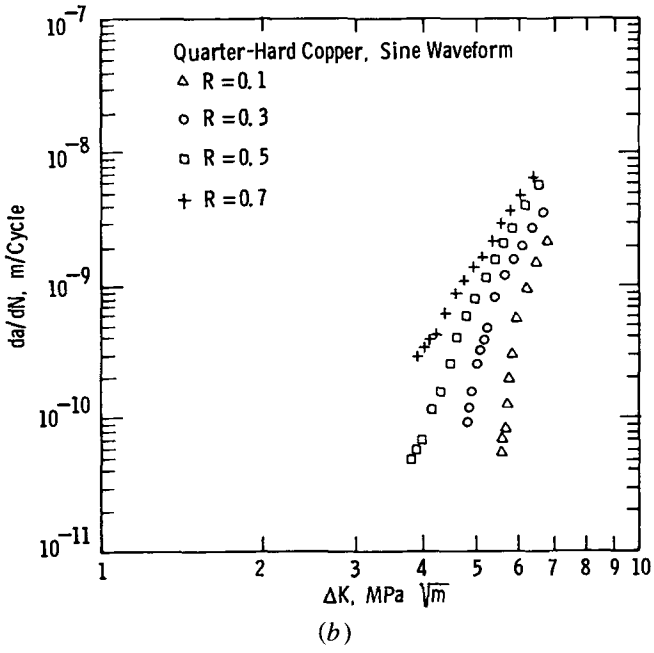

(b)

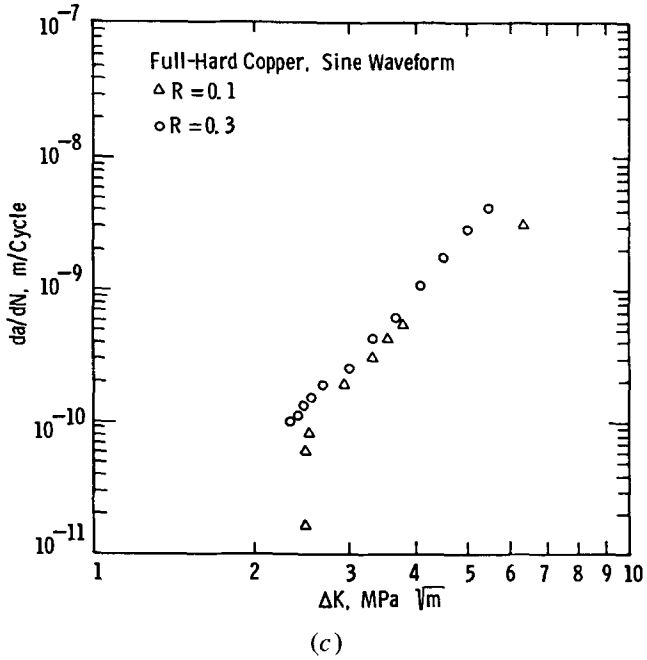

(c)

Fig. 1 — (*a*) The effect of R ratio on near-threshold crack growth rates in annealed copper. (*b*) The effect of R ratio on near-threshold crack growth rates in quarter-hard copper. (*c*) The effect of R ratio on near-threshold crack growth rates in full-hard copper.

color of the fracture surface became much darker (Figures 5(a) to (c)). This observation implies that a thick oxide layer develops at ΔK levels near the threshold. Note that a particle-like oxide was found in the threshold area, as shown in Figures 5(e) and (h) for annealed and quarter-hard copper. A detailed discussion regarding the effect of the oxide on crack growth behavior is presented later.

(b) In the region of near-threshold crack propagation, the fracture surface is a mixture of intergranular and transgranular failure regardless of material condition and R ratio (Figures 5(d), (f) to (j)). However, at the threshold, a transgranular fracture appears to be dominant (Figures 5(g), (h), and (j)).

(c) Increasing R values decreases the percentage of intergranularity and the amount of oxide. Similarly, in Ni-Cr-Mo-V,[14] Ni-Mo-V,[15] and high-purity BS 817M40[16] steels, the proportion of intergranular failure was found to decrease with an increase in R.

(d) As the value of ΔK decreases, the percentage of intergranular fracture decreases (Figures 5(i) and (j)), but the amount of the oxide increases.

(e) At a fixed value of ΔK, full-hard copper has the largest percentage of intergranular failure among the three materials (Figures 5(d) and (i)). However, during near-threshold crack growth, the full-hard material appears to have the least amount of oxide.

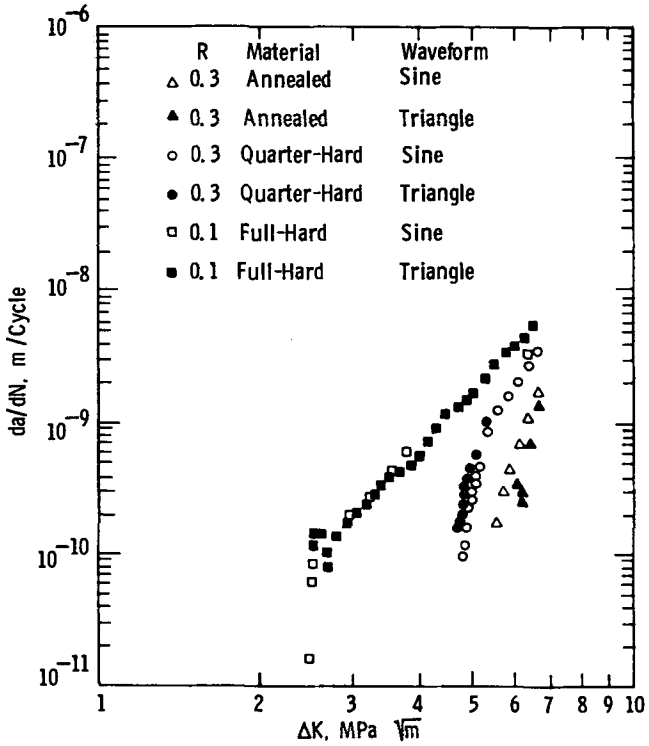

Fig. 2—The effect of waveform on near-threshold crack growth rates in copper.

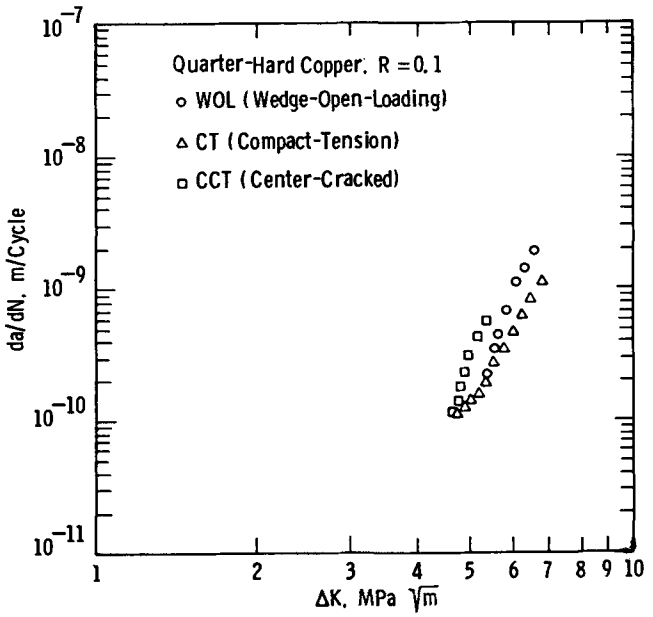

Fig. 3—The effect of specimen geometry on near-threshold crack growth rates in quarter-hard copper at $R = 0.1$.

(f) The waveform does not seem to affect the fracture morphology.

E. *Characterization of Oxide Formation in Near-Threshold Crack Growth*

As noted in Figures 5(a) to (c), (e), and (h), a large amount of oxide forms on the crack face as the crack propagation rate approaches the threshold. The same phenomenon was previously found in steels.[17–21] For a quantitative study of the oxide in the threshold crack growth, Auger spectroscopy combined with sputtering was used to determine the thickness of the oxide. The sputtering rate was calibrated to a known thickness of tantalum oxide and also by profilometry on sputtered craters. In this investigation, one minute of sputtering time corresponded to a sputtering depth of 80Å. As argon ions sputter the oxide present on the fracture surface, at. pcts of compositional elements in the oxide are periodically measured and plotted out. Consequently, we can obtain a depth profile of at. pct of oxygen *vs* the average distance, d, from the fracture surface into the oxide. Figure 6 shows the Auger results in quarter-hard copper at three R values. The at. pct of oxygen decreases with an increase in d. This is due to the fact that as Ar^+ in the Auger spectrometer continues to sputter the oxide, the amount of oxide decreases and eventually, the copper-base matrix becomes dominant.

The oxide on the fracture surfaces is probably not of exactly the same thickness within the analyzed area. Furthermore, surface roughness will affect the apparent oxygen profile measured by Auger analysis. The effect of surface roughness may be explained by considering an oxide film of uniform thickness on two types of surfaces: (a) a perfectly smooth surface, and (b) a rough surface. In case (a), the sputtering beam has a fixed orientation with respect to the oxide film, and the Auger profile will indicate a very sharp interface between oxide and base metal. In case (b), certain areas of the oxide film will be sputtered under grazing incidence, other areas under normal or near-normal incidence, and some areas will be shielded from the sputtering beam. The resulting apparent Auger profile will show a continuously decreasing level of oxygen once the oxide film has been penetrated by the sputtering beam in one area. A long tail and broad apparent interface may be typical for rough surfaces (see Figure 6 for example). The average thickness of the oxide is defined as the value of d at which the at. pct of oxygen drops 50 pct after sputtering. A similar definition was previously used by Wei and Simmons.[22] In the Auger spectrometer, the electron beam was scanned at TV-rates. The area on the fracture surface for Auger analysis was a square of 400 μm. Thus, the determined oxide thickness represents an average value in the area corresponding to a given ΔK. The average thickness of the oxide layer at various R values is listed in Table IV. At the threshold, the oxide layer thickness at $R = 0.1$ is approximately one order of magnitude greater than that at $R = 0.7$. Decreasing the R ratio increases the thickness of the oxide at the threshold level. The same results were also found in a 2.25 Cr-1 Mo pressure vessel steel.[23] In Table IV, at $R = 0.5$ the thickness of the oxide at the threshold is about ten times larger than that at a higher ΔK of 7.7 MPa $\sqrt{m}$. These quantitative measurements of the oxide thickness are in good agreement with the fractographic observations, as mentioned previously.

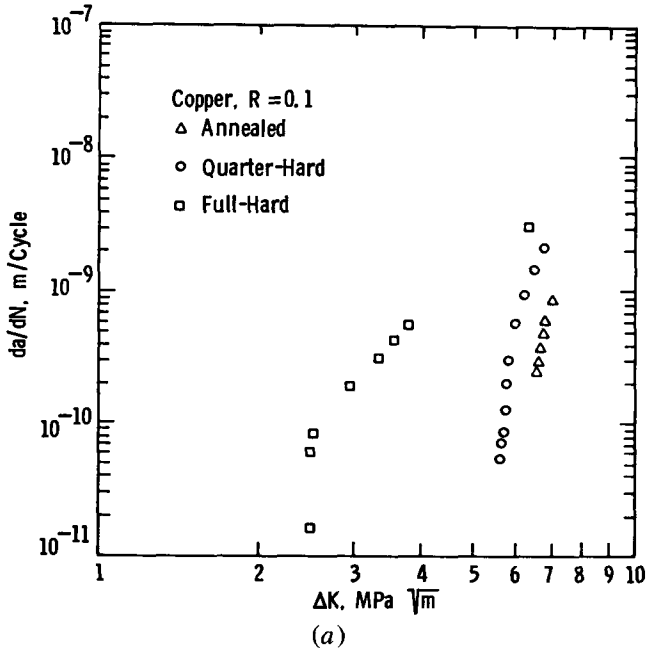

(a)

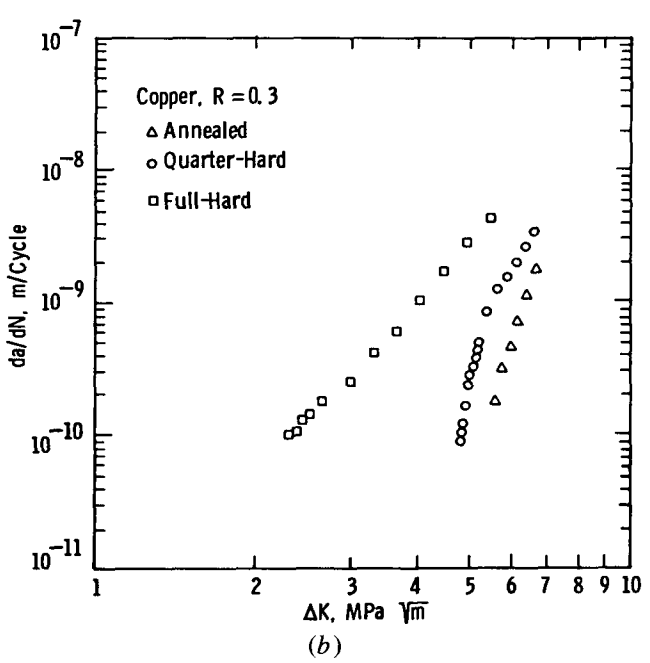

(b)

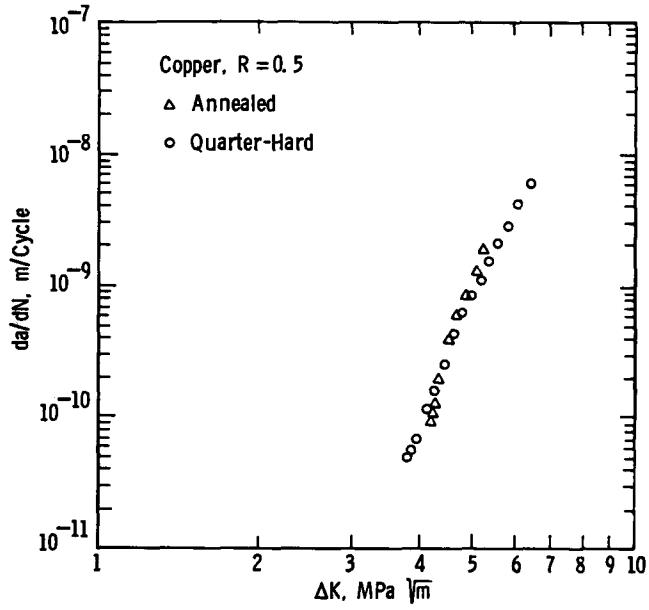

(c)

Fig. 4—(*a*) Comparison of crack growth rates in annealed, quarter-hard, and full-hard copper at $R = 0.1$. (*b*) Comparison of crack growth rates in annealed, quarter-hard, and full-hard copper at $R = 0.3$. (*c*) Comparison of crack growth rates in annealed and quarter-hard copper at $R = 0.5$.

V. DISCUSSION

The results of this investigation clearly show that increasing the R ratio significantly increases the near-threshold fatigue crack growth rates in copper. However, the influence of R values on threshold crack growth rates tends to decrease with an increase in material strength. At a lower R ratio, annealed copper has the largest value of ΔK_{th}, and the full-hard material has the smallest ΔK_{th}. Nevertheless, increasing the R ratio decreases the difference in ΔK_{th} for annealed, quarter-hard, and full-hard copper. In the following section, the effects of load ratio and material strength on threshold crack growth behavior are discussed in light of the concept of crack closure.

Table III. Values of ΔK_{th} in Copper

Material	R	ΔK_{th} MPa $\sqrt{m}$
Annealed	0.1	6.35
Annealed	0.3	5.35
Annealed	0.5	4.25
Annealed	0.7	2.95
Quarter-hard	0.1	5.70
Quarter-hard	0.3	4.85
Quarter-hard	0.5	4.10
Quarter-hard	0.7	3.30
Full-hard	0.1	2.55
Full-hard	0.3	2.35

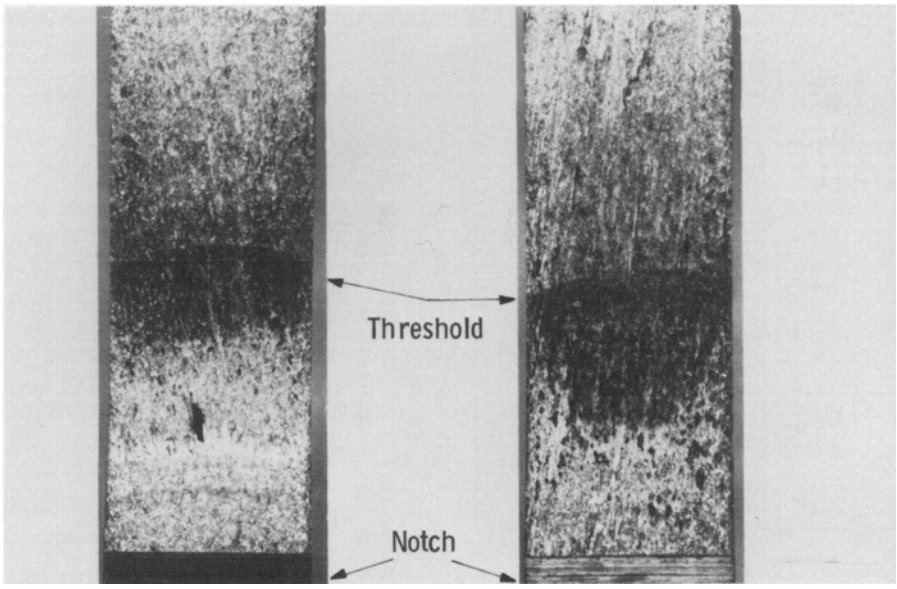

(a) (b)

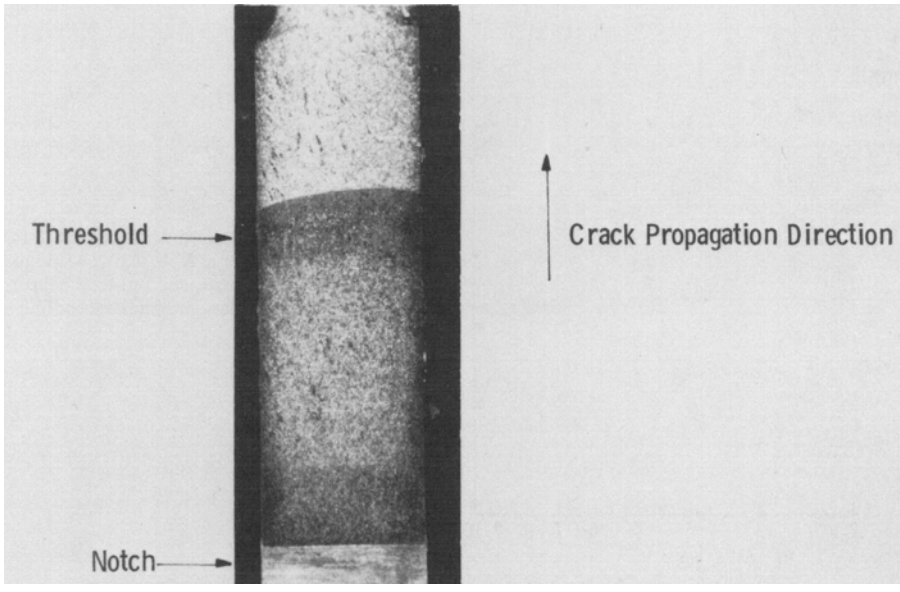

(c)

Fig. 5—(a-c) Optical photos of fracture surfaces: (a) Annealed copper, $R = 0.1$, magnification 4.3 times. (b) Quarter-hard copper, $R = 0.3$, magnification 4.3 times. (c) Full-hard copper $R = 0.1$, magnification 3.4 times.

A. *Oxide Formation*

The formation of the oxide film in near-threshold crack propagation is thought to be due to fretting oxidation[21,23] which is a process of continuously breaking and reforming of oxide. In threshold crack growth for R larger than zero, plasticity-induced crack closure, as discovered by Elber,[24] makes the upper and lower fracture surfaces contact during the tensile loading cycle, and thus, fretting occurs. It was reported that crack closure was more significant at low ΔK values than at high ΔK values.[20,25,26] Recently, Davidson,[27] and Minakawa and McEvily[28] reported that as the crack growth rate approached the threshold, Mode II crack opening (rubbing) became dominant. Fretting oxidation will be enhanced by the Mode II displacement at the threshold levels. In addition, a large number of loading cycles are imposed on a unit distance of the fracture surface, which is likely to accelerate the formation of oxide. For example, at the threshold it takes about 10^7 cycles to travel a distance of 1 mm. Consequently, decreasing ΔK in threshold crack growth enchances fretting oxidation and increases the

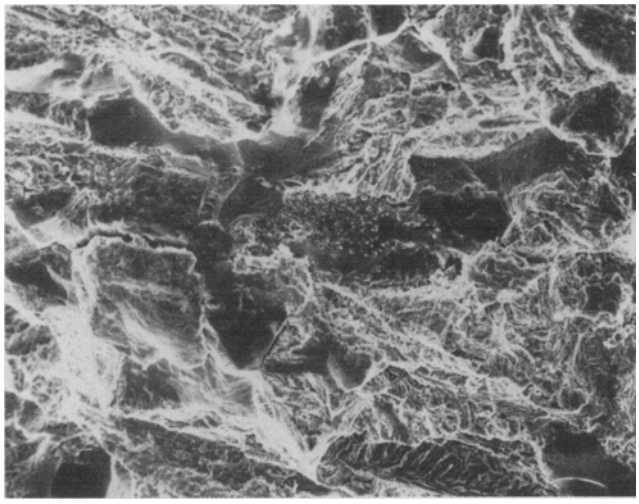

(*d*)

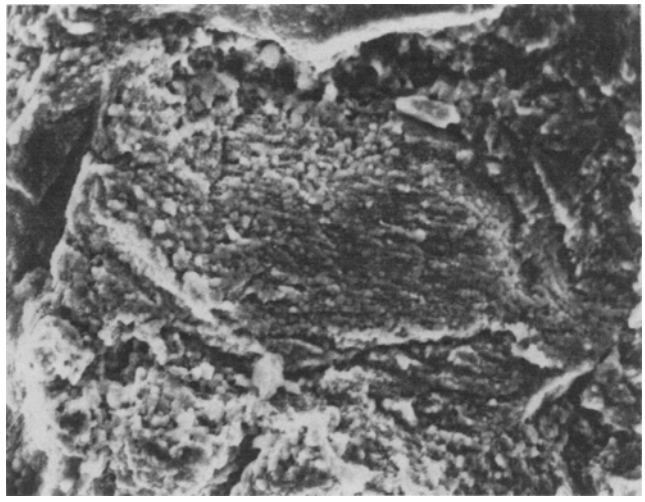

(*e*)

Crack Propagation Direction

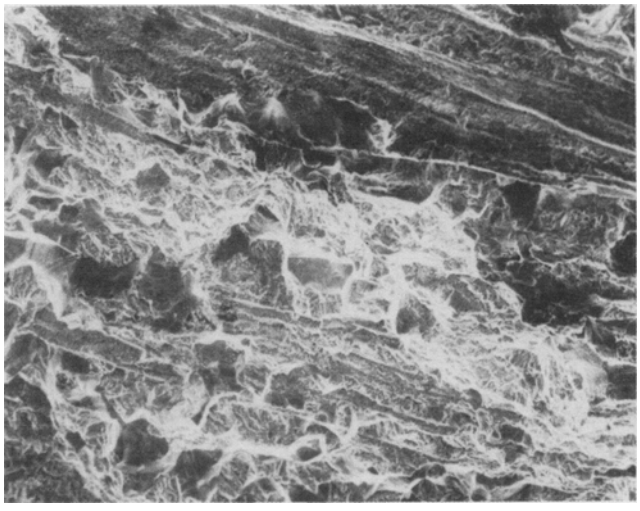

(*f*)

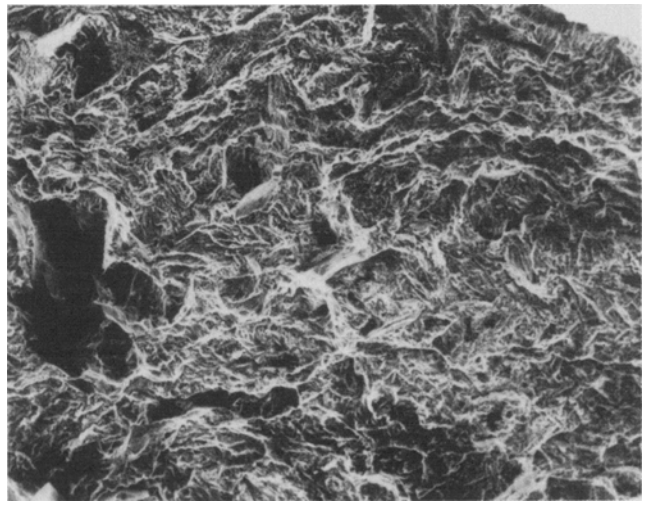

(*g*)

Fig. 5—(*d-g*) SEM photos of fracture morphology. (*d*) Annealed copper, $R = 0.1$ and $\Delta K = 7.0$ MPa $\sqrt{m}$, magnification 340 times. (*e*) Annealed copper, $R = 0.1$ at the threshold ($\Delta K = 6.35$ MPa $\sqrt{m}$), magnification 1460 times. (*f*) Annealed copper, $R = 0.3$ and $\Delta K = 6.16$ MPa $\sqrt{m}$, magnification 150 times. (*g*) Annealed copper, $R = 0.7$ at the threshold ($\Delta K = 2.95$ MPa $\sqrt{m}$), magnification 260 times.

thickness of the oxide. However, at higher R values, crack closure becomes more difficult and fretting oxidation lessens. Thus, increasing the R ratio reduces the oxide layer thickness.

X-ray diffraction study shows that the oxide in the present investigation consists of Cu_2O and CuO. CuO is the stable oxide at elevated temperature.[29] It was previously noted that the temperature rose at the fatigue crack tip.[30] Thus, it is suggested that during near-threshold fatigue crack propagation in copper, the possibly large increase of temperature due to fretting of upper and lower fracture surfaces may also promote the formation of oxide.[31]

B. *Crack Closure*

Ritchie *et al*[18,19,23] reported that the oxide present on the fracture surface enchanced crack closure in steels. They successfully used the concept of oxide-induced crack closure to explain the influence of gaseous environment on slow crack growth behavior in a 2.25 Cr-1 Mo steel. In air, a thick oxide layer exists at the threshold, which wedges the upper and lower fracture surfaces and increases the crack closure level and thus, decreases the effective stress intensity range ($\Delta K_{eff} = K_{max} - K_{closure}$). Accordingly, in the 2.25 Cr-1 Mo steel, the threshold crack growth rates in air are slower than those in the oxygen-free environment (helium or hydrogen).

In the present investigation on copper, the effect of oxide on crack closure at the threshold can be appreciated by comparing the cyclic crack opening displacement (COD) with the thickness of the oxide (d_0). In Table IV, the oxide

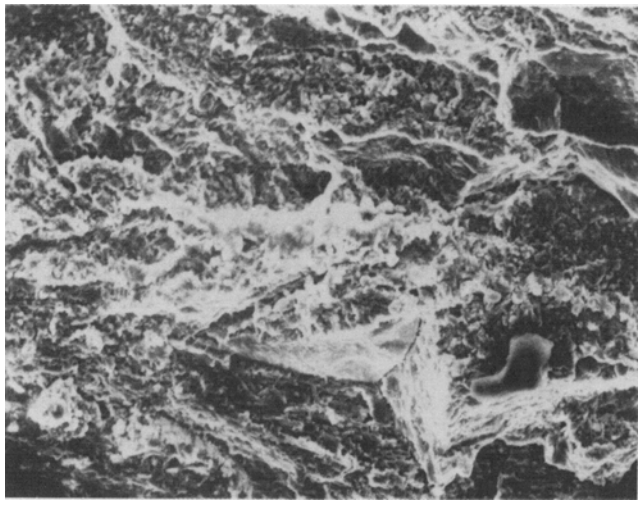

(*h*)

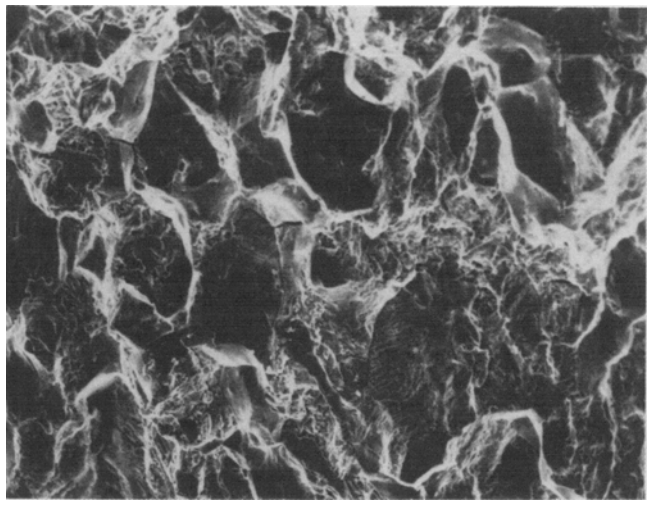

(*i*)

Crack Propagation Direction

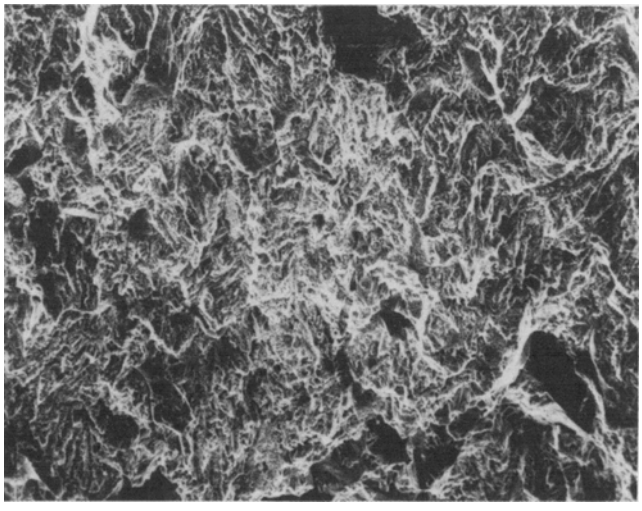

(*j*)

Fig. 5—(*h-j*) SEM photos of fracture morphology. (*h*) Quarter-hard copper, $R = 0.3$ at the threshold ($\Delta K = 4.85$ MPa $\sqrt{m}$), magnification 740 times. (*i*) Full-hard copper, $R = 0.1$ and $\Delta K = 7.15$ MPa $\sqrt{m}$, magnification 260 times. (*j*) Full-hard copper, $R = 0.1$ at the threshold ($\Delta K = 2.55$ MPa $\sqrt{m}$), magnification 260 times.

layer thickness at $R = 0.1$, 0.5, and 0.7 is 32 pct, 27 pct, and 4 pct of the value of COD, respectively. As compared to the crack opening displacement, the large amount of oxide at lower R values of 0.1 and 0.5 will wedge the crack tip to promote crack closure, as found in steels.[23] At the higher R ratio of 0.7, the influence of oxide on crack closure may be negligible due to the much thinner oxide relative to COD. Therefore, during near-threshold fatigue crack propagation, decreasing the R value increases the effect of oxide deposits on crack closure in copper. In Table IV, at $R = 0.5$, the oxide thickness and the ratio of d_0/COD at $\Delta K = 7.7$ MPa $\sqrt{m}$ are much smaller than those at the threshold. Consequently, reducing values of ΔK enhances the influence of the oxide film on crack closure in slow crack growth.

In view of the potential importance of crack closure in slow crack growth behavior, crack closure was further studied by using the strain-gage method.[32] The details of the strain-gage technique to measure the crack closure stress were reported earlier by Gan and Weertman.[32] Several strain-gages (Micro-Measurements EA-13-062AK-120), 1.57 mm wide and 1.57 mm long, were cemented on the specimen surface. While the strain-gages are approximately 5 mm apart from one another, the distance from the center of the gage to the crack plane is about 1 mm. During cyclic loading, the photos of the load *vs* strain curves were periodically taken on a Tektronix single beam storage oscilloscope. The crack closure level is determined from the change in the slope of the load *vs* strain curve. In Figure 7, the examples of the load *vs* strain curves are shown for crack closure

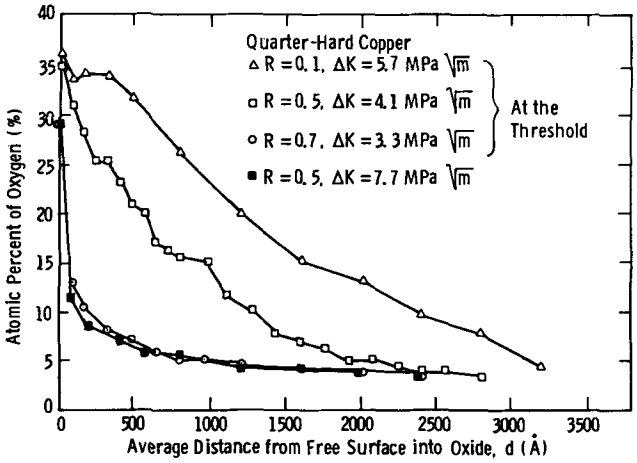

Fig. 6—Results of Auger analysis of oxide in near-threshold crack growth.

Table IV. Data of Auger Analysis and Crack Opening Displacement Associated with Near-Threshold Fatigue Crack Propagation in Quarter-Hard Copper

R	ΔK (MPa $\sqrt{m}$)	Oxide Layer Thickness, d_o Å	Cyclic Crack Opening Displacement* COD, Å	$\frac{d_o}{COD}$ (Pct)
0.1	5.7 (Threshold)	1408	4454	32
0.5	4.1 (Threshold)	624	2304	27
0.7	3.3 (Threshold)	64	1493	4
0.5	7.7	64	8128	0.8

*Cyclic crack opening displacement[18] = $0.49\ \Delta K^2/(2\ \sigma_y'\ E)$ where σ_y' is the 0.2 pct offset cyclic yield strength.

points in annealed copper at $R = 0.3$. Interestingly, at a fixed value of ΔK, varying frequency from 1 to 100 Hz does not change the crack closure level. Above the crack closure level, the slope of the load *vs* strain curve has been shown to be in good agreement with the plane stress Westergaard's elastic potential solution.[32] Thus, it should be noted that the strain-gage glued on the specimen surface may measure the plane stress crack closure level in this study.

Figure 8(a) shows the relationship between $\Delta K_{eff}/\Delta K$ *vs* ΔK at $R = 0.1$ in annealed, quarter-hard, and full-hard copper. As the value of ΔK decreases, the ratio of $\Delta K_{eff}/\Delta K$ decreases in the three materials. The same result was found in Ni-Cr-Mo-V steel.[14] This is in good agreement with the theory of Purushothaman and Tien.[26] Figure 8(a) suggests that decreasing crack growth rates increases the influence of crack closure on threshold behavior, as reported earlier.[14,25,26] In Figure 8(a), at the threshold, the value of ΔK_{eff} occupies approximately 50 pct, 54 pct, and 86 pct of ΔK in annealed, quarter-hard, and full-hard specimens, respectively. Thus, during each loading cycle, a significant portion of ΔK was spent in crack closure at the threshold levels, and crack closure needs to be considered in studying threshold crack growth behavior.

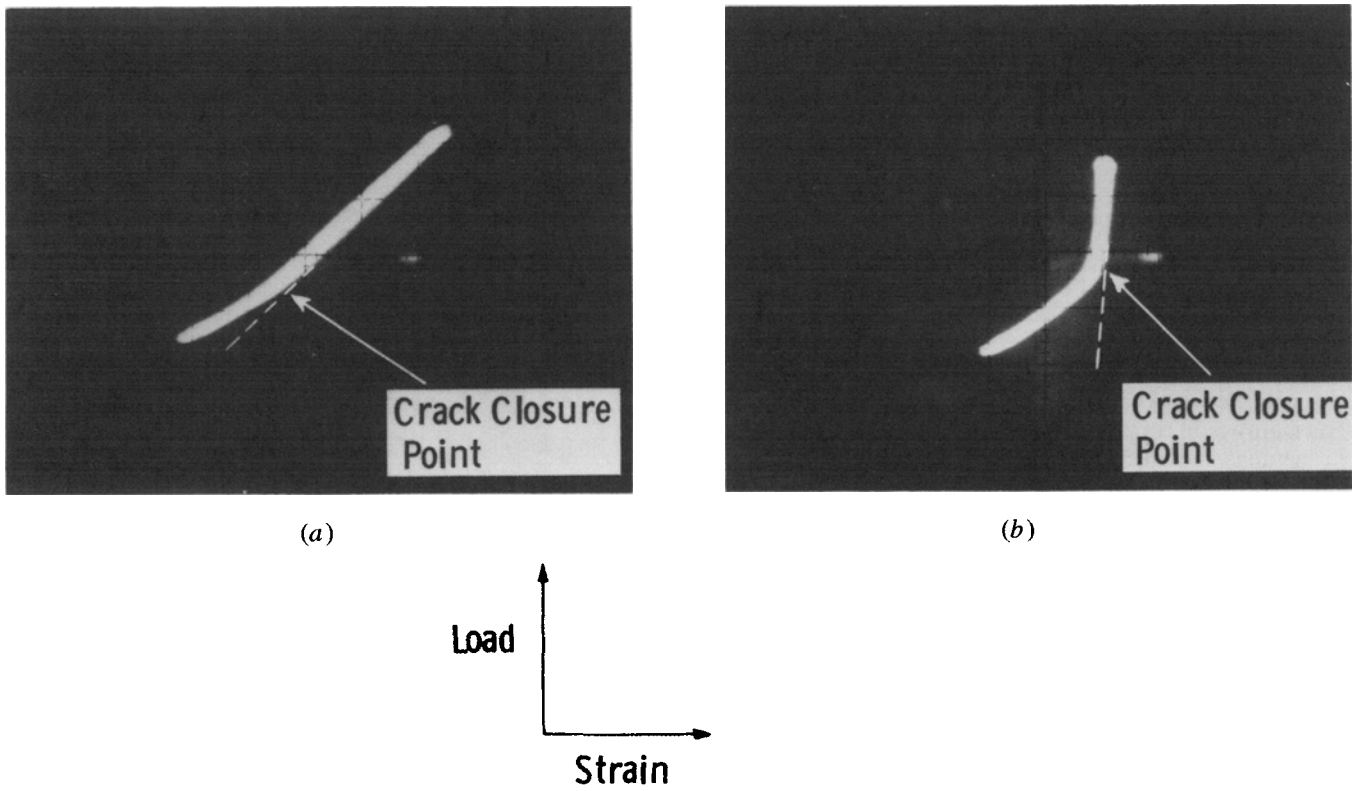

Fig. 7—Photos of load *vs* strain curves in annealed copper at $R = 0.3$. Note that the photos were taken when the strain-gage was located behind the crack tip. (*a*) $\Delta K \approx 7.0$ MPa $\sqrt{m}$; (*b*) $\Delta K \approx 6.0$ MPa $\sqrt{m}$.

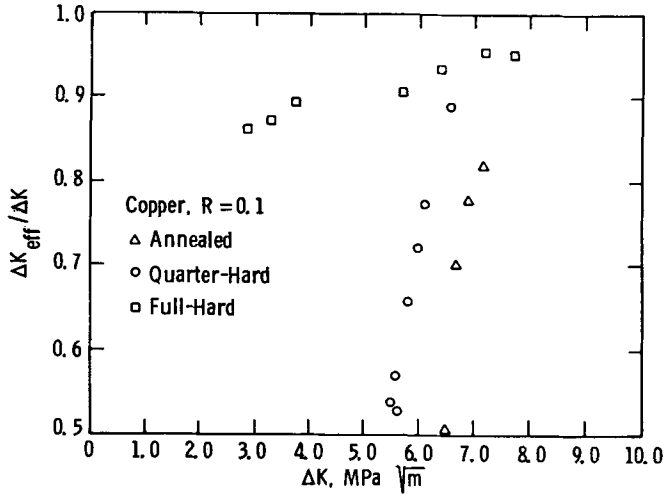

(a)

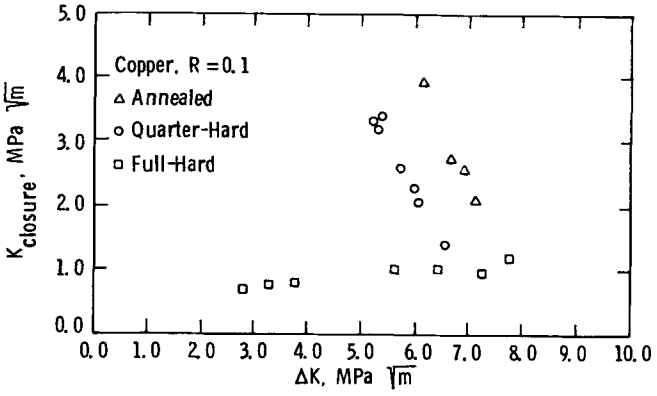

(b)

Fig. 8—(*a*) The relationship between $\Delta K_{eff}/\Delta K$ and ΔK during near-threshold crack propagation. (*b*) The relationship between $K_{closure}$ and ΔK during near-threshold crack propagation.

At a given value of ΔK, the annealed specimen has the highest crack closure level, $K_{closure}$, among the three materials while the full-hard specimen has the lowest closure level (Figure 8(b)). In full-hard copper, the lower plasticity, and the thinner oxide layer in near-threshold crack growth reduce the crack closure level, as compared to annealed and quarter-hard copper. Therefore, increasing material strength reduces the crack closure level during threshold fatigue crack growth in copper. Furthermore, large cyclic hardening in the annealed specimen may also increase the crack closure level, relative to cyclic softening in quarter-hard and full-hard specimens, which is theoretically supported by Budiansky and Hutchison.[33] In annealed and quarter-hard copper, decreasing values of ΔK increases crack closure levels (Figure 8(b)), which is related to the larger oxide thickness at lower ΔK. Independently, Minakawa and McEvily[34] found the same trend in steels and aluminum alloys. However, in their study, the increase of $K_{closure}$ at lower ΔK levels was attributed to the existence of a serrated crack path near the threshold. The mismatch and the mode II displacement of the upper and lower fracture surfaces will promote crack closure at lower ΔK values, namely, roughness-induced crack closure.[23,26,28,34-39] Roughness-induced crack closure may also play a role in this study.

In Figure 9(a), as the R ratio increases, the value of ΔK_{th} decreases for the three materials. There seems to be a linear relationship between ΔK_{th} and R in annealed and quarter-hard copper, as also reported in steels.[40] As stated earlier, at lower R values, the annealed specimen of lowest strength has the largest value of ΔK_{th} among the three materials, while the full-hard specimen of highest strength has the smallest ΔK_{th}. At higher R ratios, values of ΔK_{th} in the three materials appear to come together. Previously, Musuva and Radon[40] and Usami[41] reported the same trend in steels. If the effective threshold stress intensity range, $\Delta K_{th,eff}$, is plotted against R, it is very interesting to note that the

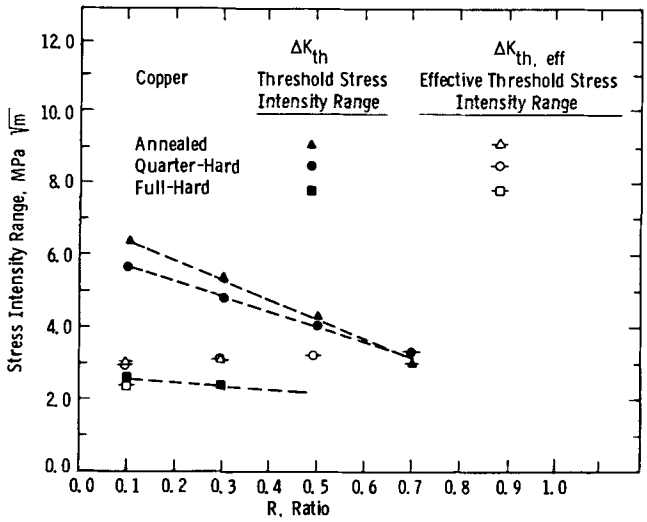

(a)

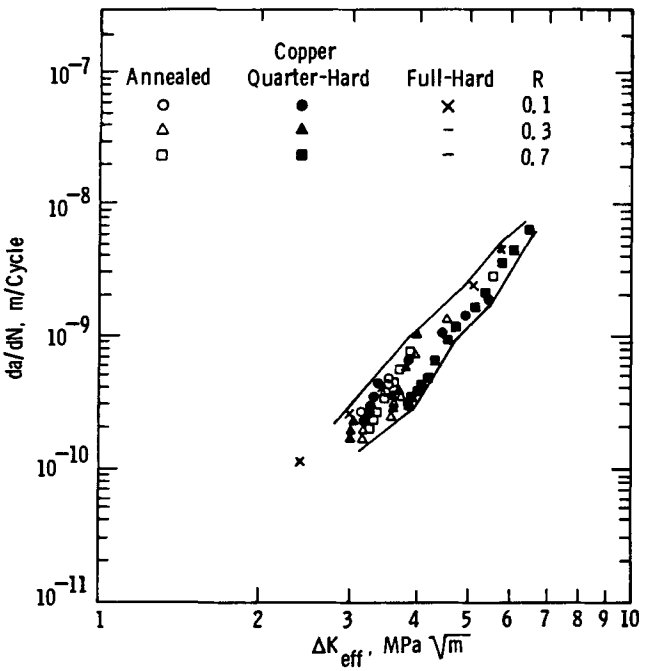

(b)

Fig. 9—(*a*) Effects of R ratios and crack closure on threshold stress intensity range. (*b*) The effect of crack closure on near-threshold crack growth rates.

values of $\Delta K_{th,eff}$ are insensitive to load ratio and material strength in annealed, quarter-hard, and full-hard specimens (Figure 9(a)). Consistently, the threshold crack propagation rate data at various R ratios for annealed or quarter-hard copper are converged to a narrow band by means of ΔK_{eff} (Figure 9(b)). Also, at a low value of R the large difference in near-threshold fatigue crack growth rates among the three materials is reduced to a minimum by using ΔK_{eff} in Figure 9(b). The same phenomenon was found in an aluminum alloy[42] and steels.[14,34,43] Thus, crack closure appears to account for the effects of load ratio and strength level on near-threshold fatigue crack propagation behavior in ETP copper.

VI. CONCLUSIONS

1. In annealed, quarter-hard, and full-hard ETP copper, increasing the R ratio increases the rates of near-threshold crack growth. As the crack propagation rate reaches the threshold, the sensitivity to R ratio effects increases.
2. The annealed specimen (lowest monotonic yield strength) has the slowest near-threshold crack growth rate among the three materials studied while the full-hard material (highest strength) has the fastest crack propagation rate. This observation implies that the near-threshold crack growth resistance increases with a decrease in material strength for ETP copper.
3. Three specimen geometries—WOL, CT, and CCT—show comparable near-threshold crack growth rate data in quarter-hard copper. Sinusoidal and triangular waveforms do not affect threshold crack propagation rates.
4. During near-threshold crack growth, the fracture morphology for all copper materials evaluated is a mixture of intergranular and transgranular fracture. As the value of ΔK decreases, the percentage of transgranular failure increases.
5. In quarter-hard copper, the thickness of the oxide film developed in the region of the fracture surface corresponding to the threshold was found to increase with a decrease in the R ratio.
6. During threshold crack propagation at $R = 0.1$, decreasing values of ΔK increases the crack closure level in annealed and quarter-hard copper, which is related to the thicker oxide at lower ΔK.
7. In annealed and quarter-hard copper, the effects of R values on near-threshold crack propagation behavior can be rationalized by crack closure. Also, at a fixed R ratio crack closure appears to account for the difference in slow crack growth rates for all three copper materials with various yield strengths.

ACKNOWLEDGMENTS

The authors are very grateful to W. G. Clark, Jr. and J. Schreurs for the critical reviews of the manuscript, and A. Saxena for kind help in planning the tests. Valuable discussions with R. O. Ritchie, N. E. Dowling, M. E. Fine, and L. D. Kunsman are greatly appreciated. We would like to thank R. E. Gainer, W. H. Halligan, R. C. Brown, A. R. Petrush, R. R. Hovan, P. J. Barsotti, D. Detar, and T. A. Manion for their help in conducting the experiments. Finally, the authors very much appreciate the financial support of Westinghouse Steam Turbine Generator Division–Generator Systems.

REFERENCES

1. C. E. Feltner and C. Laird: *Acta Met.*, 1967, vol. 15, p. 1621.
2. R. S. Williams, P. K. Liaw, M. G. Peck, and T. R. Leax: Westinghouse R&D Center, Pittsburgh, PA, unpublished research, 1981.
3. A. Saxena, S. J. Hudak, Jr., J. K. Donald, and D. W. Schmidt: *J. of Testing and Evaluation*, 1978, vol. 6, p. 167.
4. A. Saxena and S. J. Hudak, Jr.: *Int. J. Fract.*, 1978, vol. 14, p. 453.
5. R. J. Bucci, W. G. Clark, Jr., and P. C. Paris: in *Stress Analysis and Growth of Cracks*, ASTM STP 513, 1972, p. 177.
6. P. C. Paris, R. J. Bucci, E. T. Wessel, W. G. Clark, Jr., and T. R. Mager: in *Stress Analysis and Growth of Cracks*, ASTM STP 513, 1972, p. 141.
7. R. O. Ritchie: *J. Eng. Mater. Technol. Trans., ASME Series H*, 1977, vol. 99, p. 195.
8. R. J. Cooke and C. J. Beevers: *Eng. Fract. Mech.*, 1973, vol. 5, p. 1061.
9. R. J. Cooke, P. E. Irving, G. S. Booth, and C. J. Beevers: *Eng. Fract. Mech.*, 1975, vol. 7, p. 69.
10. L. P. Pook: in *Stress Analysis and Growth of Cracks*, ASTM STP 513, 1972, p. 106.
11. C. Bathias, A. Pineau, J. Pluvinage, and P. Rabbe: *Proc. of the 4th Int. Conf. on Fracture*, Waterloo, Canada, 1977, vol. 2, p. 1283.
12. S. J. Hudak, Jr., A. Saxena, R. J. Bucci, and R. C. Malcolm: Development of Standard Methods of Testing and Analyzing Fatigue Crack Growth Data, Final Report, March 1978, Air Force Materials Lab. Contract F 33615-75-C-5064, Westinghouse Research Labs, Pittsburgh, PA.
13. R. O. Ritchie: *International Metals Review*, 1979, vol. 20, p. 205.
14. P. K. Liaw, S. J. Hudak, Jr., and J. K. Donald: *Metall. Trans. A*, 1982, vol. 13A, p. 1633.
15. P. K. Liaw, S. J. Hudak, Jr., and J. K. Donald: 14th National Symposium on Fracture Mechanics, ASTM, STP, 1981, in press.
16. P. E. Irving and A. Kurzfeld: *Metal Science*, 1978, vol. 12, p. 495.
17. R. O. Ritchie, S. Suresh, and C. M. Moss: *J. Eng. Mater. Technol., Trans., ASME Series H*, 1980, vol. 102, p. 293.
18. R. O. Ritchie: Proceedings of the Intl. Conf. on "Analytical and Experimental Fracture Mechanics", Rome, June 1980, G. C. Sih, ed., Sijthoff and Noordhoff, The Netherlands, p. 81.
19. S. Suresh, G. F. Zamiski, and R. O. Ritchie: *In the Application of 2-1/4 Cr-1 Mo Pressure Vessel Steel for Thick-Wall Pressure Vessels*, ASTM STP, 1980, in press.
20. A. T. Stewart: *Eng. Fract. Mech.*, 1980, vol. 13, p. 463.
21. D. Benoit, R. Namdar-Tixier, and R. Tixier: *Mater. Sci. Eng.*, 1980, vol. 45, p. 1.
22. R. P. Wei and G. W. Simmons: Fracture Mechanics and Surface Chemistry Studies of Steels for Coal Gasification Systems, 1978, Second annual report, Lehigh University, Bethlehem, PA.
23. S. Suresh, G. F. Zamiski, and R. O. Ritchie: *Metall. Trans. A*, 1981, vol. 12A, p. 1435.
24. W. Elber: in *Damage Tolerance in Aircraft Structures*, ASTM STP 486, 1971, p. 230.
25. A. J. McEvily: *Metal Science*, 1977, vol. 11, p. 274.
26. S. Purushothaman and J. K. Tien: 5th Conference on the Strength of Metals and Alloys, Proc. ICSMA5 Conf., Pergamon Press, New York, NY, 1979, vol. 2, p. 1267.
27. D. L. Davidson: *Fatigue of Engineering Materials and Structures*, 1980, vol. 3, p. 229.
28. K. Minakawa and A. J. McEvily: *Scripta Met.*, 1981, vol. 15, p. 633.
29. C. L. Mantell: *Engineering Materials Handbook*, McGraw-Hill Co., New York, NY, 1958, section 36, p. 41.
30. R. Attermo and G. Ostberg: *Int. J. of Fract. Mech.*, 1971, vol. 7, p. 122.
31. L. D. Kunsman: Westinghouse R&D Center, Pittsburgh, PA, private communication, January 1981.
32. D. Gan and J. Weertman: *Eng. Fract. Mech.*, 1981, vol. 18, p. 87.
33. B. Budiansky and J. W. Hutchinson: *J. of Applied Mechanics*, 1978, vol. 45, p. 267.

34. K. Minakawa and A. J. McEvily: in *Fatigue Thresholds, Proceedings 1st Intl. Conf.*, Stockholm, J. Backlund, A. Blom, and C. J. Beevers, eds., EMAS publ. Ltd., Warley, U. K., 1981.
35. R. O. Richie: *ibid.*
36. I. C. Mayes and T. J. Baker: *Metal Science,* 1981, vol. 15, p. 320.
37. R. J. Cooke and C. J. Beevers: *Mat. Sci. and Eng.*, 1974, vol. 13, p. 201.
38. G. T. Gray, A. W. Thompson, J. C. Williams, and D. H. Stone: in *Fatigue Thresholds, Proceedings 1st Intl. Conf.*, Stockholm, J. Backlund, A. Blom, and C. J. Beevers, eds., EMAS publ. Ltd., Warley, U. K., 1981.
39. G. T. Gray: Ph.D. Thesis, Carnegie-Mellon University, Pittsburgh, PA 15213, 1981.
40. J. K. Musuva and J. C. Radon: *5th International Conference on Fracture,* D. Francois, ed., Pergamon Press, Cannes, France, 1981, vol. 3, p. 1365.
41. S. Usami: in *Fatigue Thresholds, Proceedings 1st Intl. Conf.*, Stockholm, J. Backlund, A. Blom, and C. J. Beevers, eds., EMAS publ. Ltd., Warley, U. K., 1981.
42. R. A. Schmidt and P. C. Paris: in *Progress in Flaw Growth and Fracture Toughness Testing,* ASTM STP 536, 1973, p. 79.
43. Y. Nakai, K. Tanaka, and T. Nakanishi: *Eng. Fract. Mech.*, 1981, vol. 15, p. 291.